PAFTA BELT BUCKLE VI-64513 - CU ZN ALLOY - 19TH CENTURY

Artefact name Pafta belt buckle VI-64513

Authors Inès. Golay (HE-ARC CR, Neuchâtel, Neuchâtel, Switzerland)

Url /artefacts/1616/

The object



Credit HE-Arc CR, I.Golay.

Fig. 1: General view of the front face of the belt buckle,

This work is licensed under CC BY-NC-ND 4.0



Fig. 2: General view of the back face of the belt buckle,

Credit HE-Arc CR, I.Golay.

Description and visual observation

Description of the artefact	Belt buckle of the so-called “pafta” type, consisting of two trapezoidal elements connected by a hinge and pin mechanism. The pin is attached to the left element by a chain. One of the two elements conceals the hinge behind a rectangular plate adorned with three cabochons set with colored glass stones. The central stone is green, and the other two are red. Both parts are decorated in the same manner, with stylized plant motifs. The motif consists of four sections separated by white and blue lines. It is executed using the filigree technique with black, yellow, white, blue, and green enamel. Some of the enameled areas have been painted. Red paint is applied over the yellow enamel in most places; otherwise, the paint is a color similar to that of the underlying enamel (black, white, blue). Dimensions: Width = 5.5cm, Length = 14.5cm, High = 0.8cm.
Type of artefact	clothing element
Origin	Eastern Europe
Recovering date	Date unknown
Chronology category	19th century
chronology tpq	1780 A.D.
chronology taq	1840 A.D.
Chronology comment	
Burial conditions / environment	Indoor atmosphere
Artefact location	Museum der Kulturen, Basel, Basel-City
Owner	Museum der Kulturen, Basel, Basel-City

This work is licensed under CC BY-NC-ND 4.0

Inv. number	VI-64513
Recorded conservation data	N/A

Complementary information

The object was stored for many years (between 1990 and 2010) on a wooden shelf in the museum's former storage facilities, located beneath Münsterplatz in Basel. Biocide treatments (the exact nature of which is unknown) were carried out in these facilities to prevent insect infestation. The last treatment of this kind took place in 1999.

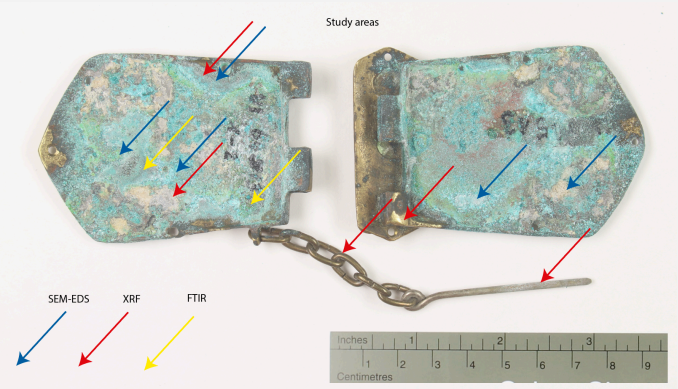
The object is now stored in the museum's new storage facilities, where the temperature is maintained at approximately 19 °C and the relative humidity at 50%. It is placed on a metal rolling shelf, inside an acid-free cardboard box, with a small piece of polyethylene foam underneath.

Study area(s)



Credit HE-Arc CR, I.Golay.

Fig. 3: Location of the study areas on the front face of the belt buckle,



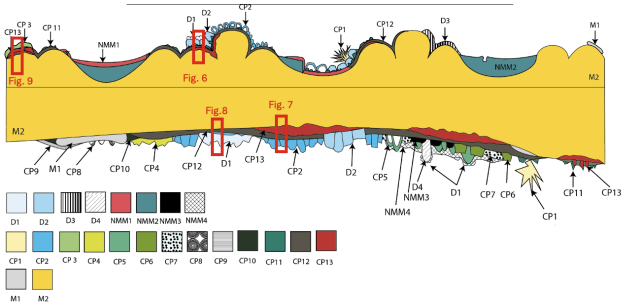
Credit HE-Arc CR, I.Golay.

Fig. 4: Location of the study areas on the back face of the belt buckle,

Binocular observation and representation of the corrosion structure

The schematic representation below gives an overview of the corrosion structures encountered on the belt buckle from a first visual macroscopic observation.

This work is licensed under CC BY-NC-ND 4.0



D1	White corrosion in the form of small powdery particles observed during the examination of the object (Trihydrated sodium acteate)	CP5	Light green corrosion, hard and in form of little sphere and bubbles
D2	Big crystals semi-transparent lightly turquoise	CP6	Green corrosion in the shape of small squares
D3	Whitish deposit	CP7	White corrosion under the varnish
D4	Big transparent crystal	CP8	Little white dots in lines on the grey metal
NMM1	Paint	CP9	White yellowish corrosion in form of little crystals/powder
NMM2	Enamel	CP10	Dark Green and hard corrosion
NMM3	Ink of the N°Inv	CP11	Fir tree green corrosion in form of little crystals and spheres
NMM4	Varnish of the N°Inv	CP12	Brown-green greyish corrosion, flat, thin and hard
CP1	White corrosion in form of needles	CP13	Orange-red corrosion lightly crumbly
CP2	Light green/ turquoise corrosion hard and in form of spheres and bubbles	M1	Brazing metal
CP3	Green corrosion in form of round little plates	M2	Brass Metal
CP4	White-yellowish corrosion in form of semi-transparent crystals		

Credit HE-Arc CR, I.Golay.

Fig. 5: Stratigraphic representation of the corrosion structure of the belt buckle by macroscopic and binocular observation (top: front; bottom: back) with reference to Figs. 6 to 9,

MiCorr stratigraphy(ies) – Bi

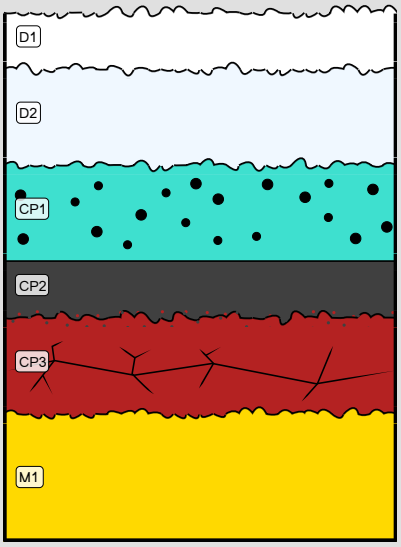


Fig. 6: Stratigraphic representation of the corrosion structure of the belt buckle observed macroscopically under binocular microscope using the MiCorr application with reference to Fig. 5. The characteristics of the strata are accessible by clicking on the drawing that redirects you to the search tool by stratigraphy representation. CP13, CP12 and CP2 in Fig. 5 are CP3, CP2 and CP1, Credit HE-Arc CR, I.Golay.

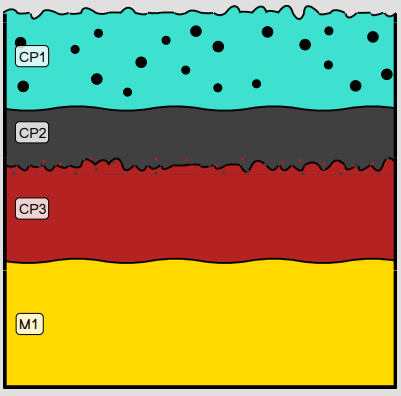


Fig. 7: Stratigraphic representation of the corrosion structure of the belt buckle observed macroscopically under binocular microscope using the MiCorr application with reference to Fig. 5. The characteristics of the strata are accessible by clicking on the drawing that redirects you to the search tool by stratigraphy representation. This stratigraphy represent the main corrosion type we find on the objet. CP13, CP12 and CP2 in Fig. 5 are CP3, CP2 and CP1, Credit HE-Arc CR, I.Golay.

This work is licensed under CC BY-NC-ND 4.0

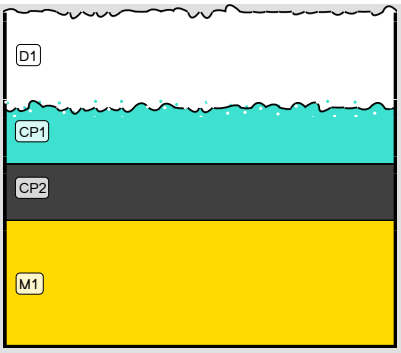


Fig. 8: Stratigraphic representation of the corrosion structure of the belt buckle observed macroscopically under binocular microscope using the MiCorr application with reference to Fig. 5. The characteristics of the strata are accessible by clicking on the drawing that redirects you to the search tool by stratigraphy representation. CP12 and CP2 in Fig. 5 are CP2 and CP1, Credit HE-Arc CR, I.Golay.

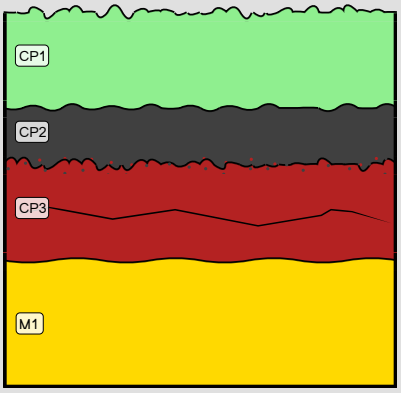


Fig. 9: Stratigraphic representation of the corrosion structure of the belt buckle observed macroscopically under binocular microscope using the MiCorr application with reference to Fig. 5. The characteristics of the strata are accessible by clicking on the drawing that redirects you to the search tool by stratigraphy representation. Green corrosion products are found ponctually on the front and the back faces. CP13, CP12 and CP3 in Fig. 5 are CP3, CP2 and CP1, Credit HE-Arc CR, I.Golay.

Sample(s)

Description of sample	None.
Alloy	Cu Zn alloy
Technology	Cast, cold worked, brazed and enamelled
Lab number of sample	
Sample location	None
Responsible institution	None
Date and aim of sampling	

Complementary information

None.

Analyses and results

Analyses performed:

Non-invasive approach

XRF with handheld portable X-ray fluorescence spectrometer (NITON XL5). General Metal mode, acquisition time 60s (filters: Li20/Lo20/M20).

Invasive approach

This work is licensed under CC BY-NC-ND 4.0

- Scanning Electron Microscopy /Energy Dispersive X-ray Spectrometry (SEM-EDS) on corrosion powder samples. Samples was prepared by scraping of material from the surface with scalpel under binocular microscope. The sample material was attached to steel pins with double sided carbon tape. Analyses were performed with a Jeol JSM-6400 device, 20,0 kV, x5k.
- FTIR: ATR mode, range 4000–675 cm^{-1}, spectral resolution 4 cm^{-1}.

Non invasive analysis

The metal is made of copper and zinc mostly (brass). Tin, iron, lead and antimony are in lower percentage.

Elements	Cu	Zn	Sn	Fe	Pb	Sb
Mass%	72	25	<1	<1	<0.5	<0.5

Table 1: Chemical composition of the metal. Method of analysis: HE-Arc portable XRF.

The metal surface can be scratched with a stainless steel scalpel. No microstructure could be observed on the metal surface.

Metal

The metal itself has not been analysed.

Microstructure Unknown

First metal element Cu

Other metal elements Zn, Sn, Sb, Pb, Fe

Complementary information

None.

Corrosion layers

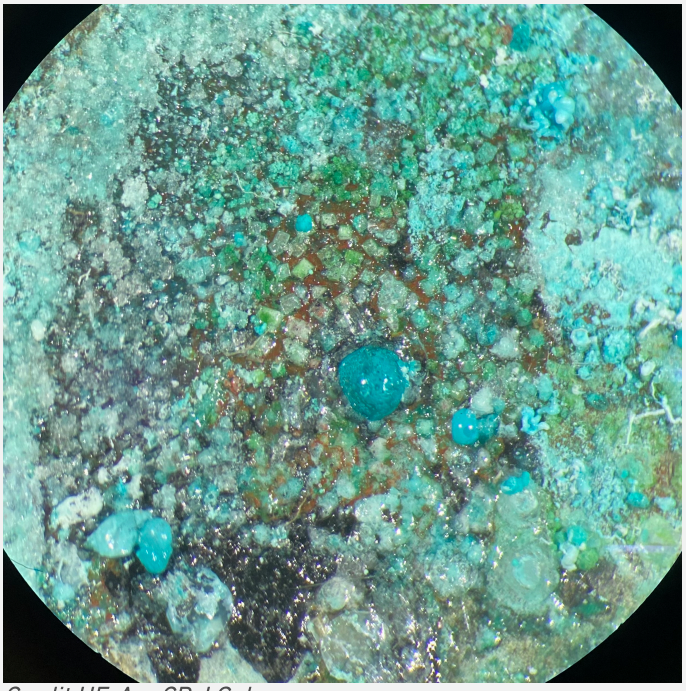
The corrosion is highly heterogeneous, generally porous and reactive. The metal is partly covered by a very porous and somewhat brittle red corrosion layer (CP13), on which there are hard light green (CP3), dark green (CP5 and CP6) and turquoise corrosion products in the form of plates, bubbles, small spheres or fine crystals (CP2) (Fig. 10). The other part of the corroded metal is covered by a thin, hard black corrosion layer (CP 12); on which dark green crystals develop (CP11), turning turquoise and taking on a bubble-like shape as they grow larger (CP2) (Fig. 11 and 12). SEM-EDS analysis indicates a high proportion of Zn as well as Na and Cl. In two zones where this corrosion develops, white, brittle needle-like corrosion was found (CP1) (Fig. 13).

In some areas of the black corrosion, the crystals are not green but translucent blue (Fig. 14). In the space of an afternoon, these turned into a white, powdery corrosion product in the form of small balls that dissolved instantly on contact with water (D1) (Fig. 15). With the FTIR analysis we found out that it is trihydrated sodium acetate (Fig. 16).

The surface is also partly covered with large translucent crystals, sometimes blue, sometimes green and sometimes yellowish (D2). They are not very hard, do not adhere well and have the texture of grains of salt (Fig. 17). SEM-EDS analysis of these grains shows the presence of sodium and chlorine (Fig. 18).

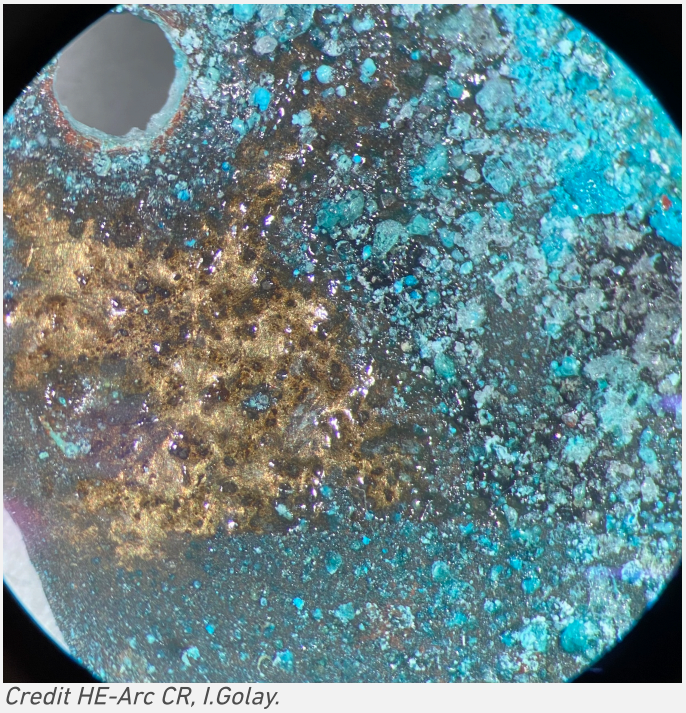
This work is licensed under CC BY-NC-ND 4.0

Traces of solder metal (M2) can be found in a few areas beneath the buckle. These are also often covered with very brittle, yellowish-white corrosion products in the form of fine crystals (CP4) (Fig. 19), and in some cases the metal is partially covered with small white crystals (CP8) (Fig. 20). Around these yellowish-white corrosion products, another type of corrosion product can be seen in the form of a thin, dark green, fairly hard ring (CP10).



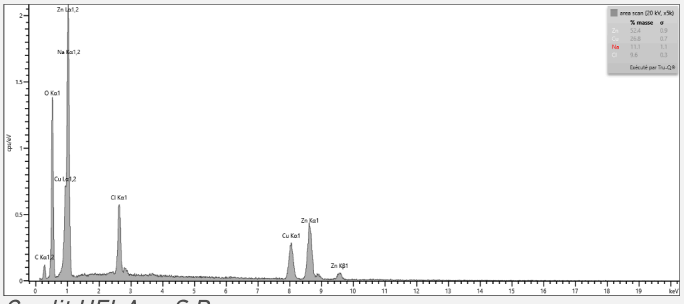
Credit HE-Arc CR, I.Golay.

Fig. 10: Green and turquoise corrosion products. Zoom 40x,



Credit HE-Arc CR, I.Golay.

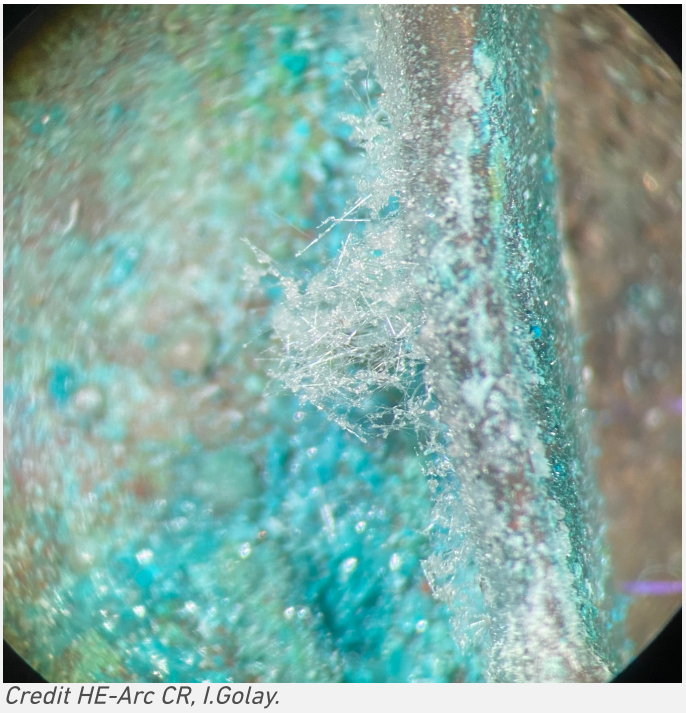
Fig. 11: Black, thin green and turquoise corrosion products. Zoom 40x,



Credit HEI-Arc, S.Ramseyer.

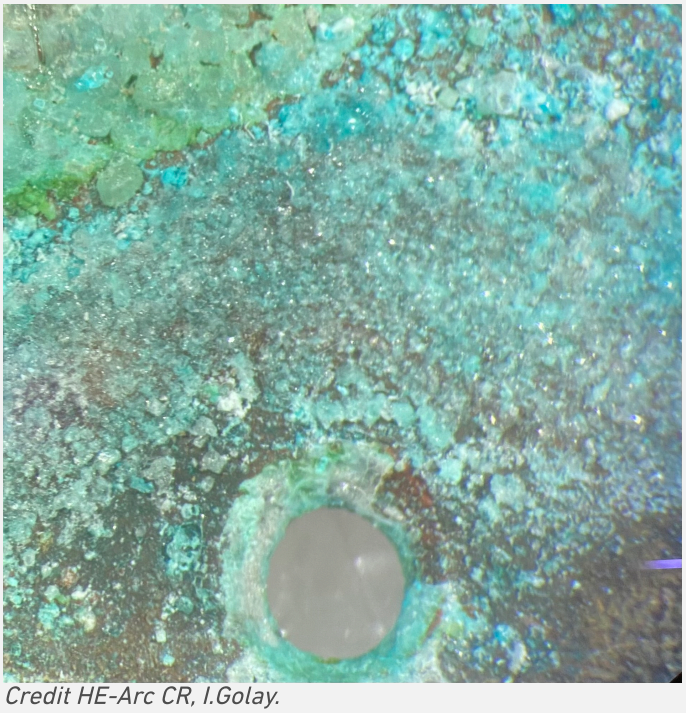
Fig. 12: SEM-EDS spectra of the turquoise blue corrosion product.

This work is licensed under CC BY-NC-ND 4.0



Credit HE-Arc CR, I.Golay.

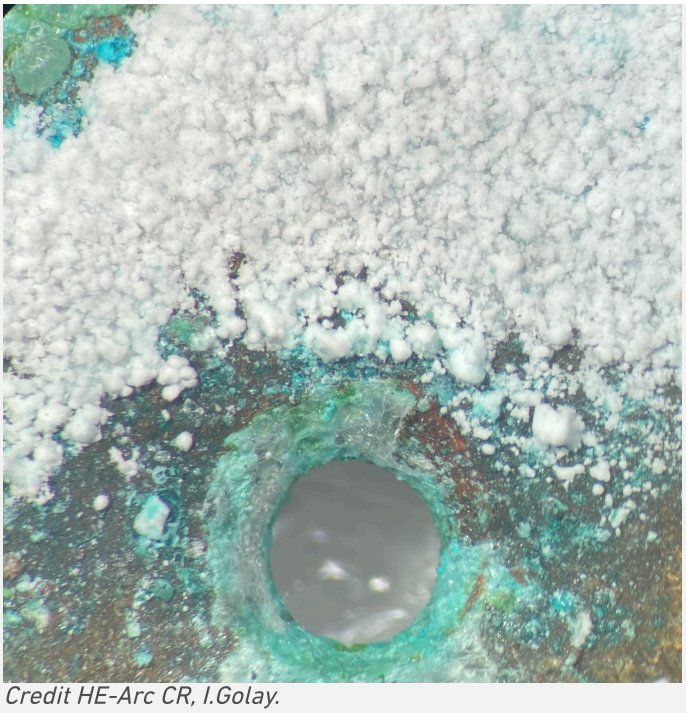
Fig. 13: White needle-like corrosion. Zoom 40x,



Credit HE-Arc CR, I.Golay.

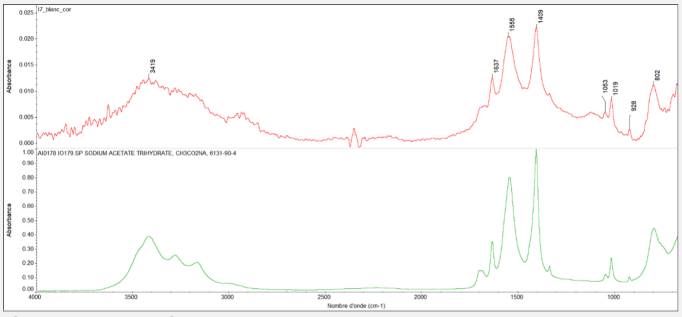
Fig. 14: Blue translucent corrosion product before change of state. Zoom 40x,

This work is licensed under CC BY-NC-ND 4.0



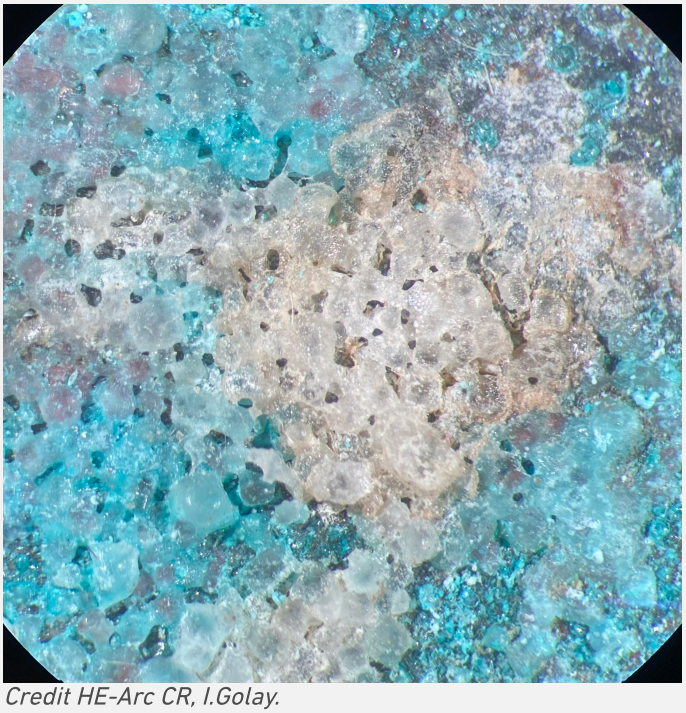
Credit HE-Arc CR, I.Golay.

Fig. 15: White brittle corrosion product after change of state. Zoom 40x,



Credit HE-Arc CR, E.Joseph.

Fig. 16: FTIR spectra of the white brittle corrosion product.



Credit HE-Arc CR, I.Golay.

Fig. 17: White-yellowish and turquoise big crystals in form of salt grain. Zoom 40x,

This work is licensed under CC BY-NC-ND 4.0

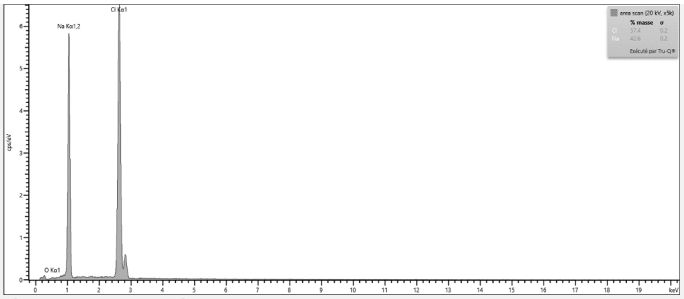


Fig. 18: SEM-EDS spectra of the white-yellowish big crystals in form of salt grain,

Credit HEI-Arc, S.Ramseyer.

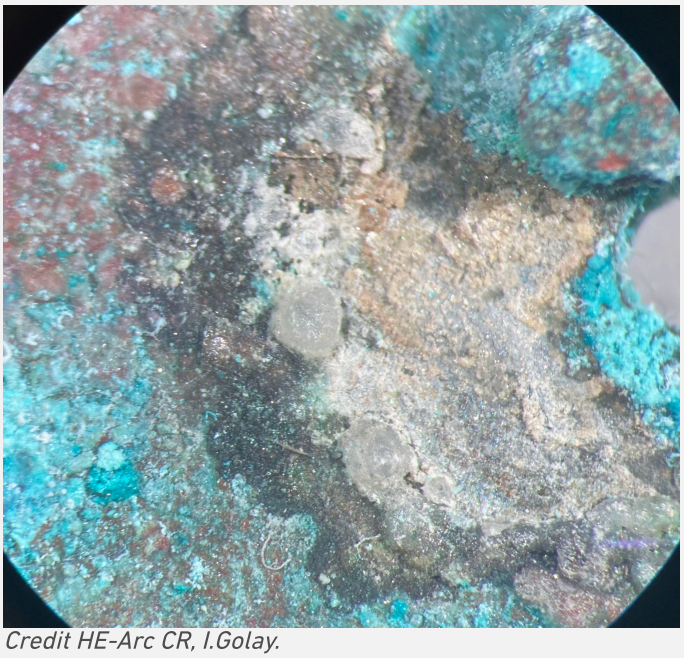


Fig. 19: White-yellowish and dark green corrosion products on the solder metal. Zoom 40x,

Credit HE-Arc CR, I.Golay.

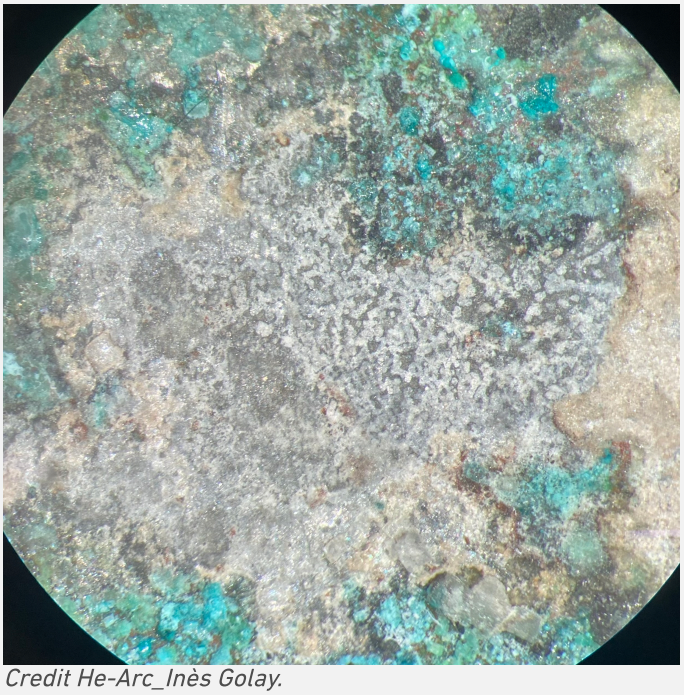


Fig. 20: White dots corrosion product on the solder metal. Zoom 40x,

Credit He-Arc_Inès Golay.

Corrosion form	Multiform
Corrosion type	Dezincification

This work is licensed under CC BY-NC-ND 4.0

Complementary information

During the treatment of the object, after the corrosion was removed, the exposed metal surface was a coppery pink color. It was therefore concluded that the surface had undergone selective zinc corrosion. Furthermore, the analyses showed a composition of approximately 72/25 Cu-Zn, which corresponds to a brass alloy susceptible to dezincification, according to Selwyn, 2004, pp. 59 and 77.

MiCorr stratigraphy(ies) – CS

Synthesis of the binocular / cross-section examination of the corrosion structure

Conclusion

The belt buckle exhibits a very surprising corrosion pattern, with numerous corrosion products and deposits of various shapes. The cause of this corrosion is likely multifactorial. First, there is the presence of sodium and chlorine salts. The origin of these salts on the object could be perspiration from wearing the buckle, residues from a previous, poorly rinsed treatment (sesquicarbonate), or even biocides intended for organic materials, present in the environment and deposited on the buckle. Furthermore, variations in humidity and the presence of acidic, acetate-based pollutants in the immediate environment of the object during its many years of storage on a wooden shelf in the museum's depots have caused specific forms of corrosion.

References

References on object and analytical methods

Reference on object

1. Ihrig, B. (1992) Theorien und Konzepte zur Bronzekonservierung von 1860 bis Beginn der 40er Jahre Methoden und Materialien zu Zeiten Rathgens. Diplomarbeit. Stuttgart: Institut für Museumkunde an der Staatlichen Akademie der Bildenden Künste.
2. Scott, D.A. (2003) Copper and bronze in art: corrosion, colorants, conservation. Los Angeles: Getty conservation institute. ISBN 978-0-89236-638-5.
3. Selwyn, L. (2004) Métaux et corrosion: un manuel pour le professionnel de la conservation. Ottawa: Institut canadien de conservation. ISBN 978-0-662-77743-4.

Reference analytical methods

4. Tennent, N.H and Baird, T. (1992) The identification of acetate efflorescence on bronze antiquities stored in wooden cabinets, The Conservator, vol. 16, no 1, pp. 39-47. DOI 10.1080/01400096.1992.9635625.

This work is licensed under CC BY-NC-ND 4.0